# Supplementary Appendix

Supplement to: Pierce EA, Aleman TS, Jayasundera KT, et al. Gene editing for *CEP290*-associated retinal degeneration. N Engl J Med 2024;390:1972-84. DOI: 10.1056/NEJMoa2309915

This appendix has been provided by the authors to give readers additional information about the work.

**Supplementary Appendix 1**

## Gene-editing for *CEP290*-associated Retinal Degeneration

Pierce EA, Aleman TS, Jayasundera KT, Ashimatey BS, Kim K, Rashid A *et al.*

**Table of Contents**

**BRILLIANCE Clinical Trial Sites and Personnel**

Personnel are listed as (I) for Study Investigator, (C) for Coordinator, (O) Ophthalmic Technician, (Ph) for Pharmacist, and (P) for Photographer.

| Clinical Trial Site | Personnel |
|---|---|
| Mass Eye and Ear (Boston, MA) | Eric A. Pierce MD PhD (I)*, Jason Comander MD PhD (I), Rachel Huckfeldt MD PhD (I), Dean Eliott MD (I), Kevin Ferenchak MD ( I), Brian Ballios MD PhD (I), Sarah Chorfi MD (I), Priya Gupta MD (I), Osama Sorour MD (I), Carol Weigel (C), Shyana Harper (C), Xiao-Hong Wen (C), Mirjana Nordmann (C), Tony Succar (C), Tu Doan (C), Yuki Wiland (C), Adey Negasa (C), Valerie Palmer (C), Devon McIsaac (C), Aditya Raj (C), My Nguyen (C), Christine Finn (Ph), Michael Zdzieblo (Ph), Judy Yee (Ph), Bethany Biron (O), Yuji Che (O), Jasmeet Bhullar (O), Emorfily Potsidis (O), Maria Escalante Gutierrez (C & O), John Hensel (P), Sarah Brett (P), Lisa Dennehy (P), Matthew DiRocco (P), Michael Krigman (P), Jean Larkin (P) |
| Bascom Palmer Eye Institute (Miami, Florida) | Byron L. Lam MD (I), Ninel Z. Gregori MD (I), Potyra Rosa (C), Adriana Drada (C), Osmany Gil Figueredo (O), Mu Liu (O), Miguel Valladares Regalado (O) Brandon Sparling (P). |
| Casey Eye Institute (Portland, Oregon) | Mark E Pennesi MD PhD (I), Paul Yang MD PhD (I), Lesley Everett MD PhD (I), Ednah Louie (C), Mary (Maggie) Ryan PharmD BCPPS (Ph), Benel Ostin (O), Darius Liseckas (O), Evan Childers (O), Erik Anaya (O) |
| W.K. Kellogg Eye Center (Ann Arbor, Michigan) | Kanishka T. Jayasundera, MD (I), Abigail T. Fahim, MD, PhD (I), Naheed W. Khan, PhD (I), Kari Branham, MS (I), Dana Schlegel, MS (I), Abby Sharp, BS, COA, CCRP (C), Callie Gordon, COA, CCRP, (C), Munira Hussain, MS, CCRP (C), Sonya Cosby (P) |
| Scheie Eye Institute at the Children's Hospital of Philadelphia and the Hospital of the University of Pennsylvania (Philadelphia, Pennsylvania) | Tomas S. Aleman MD (I), Albert M. Maguire (I), Kelsey M. Parchinski (P), Arlene J. Santos (O), Mariejel L. Weber (C) |

* Senior Investigator

**Supplementary Methods**

*Study design*

This phase 1/2 open-label, single ascending dose trial was conducted in accordance with the principles of Good Clinical Practice and the Declaration of Helsinki. Institutional review board approval was obtained at each of the five trial sites, which included Bascom Palmer Eye Institute (Miami, Florida), Massachusetts Eye and Ear Infirmary (Boston, Massachusetts), W.K. Kellogg Eye Center (Ann Arbor, Michigan), Casey Eye Institute (Portland, Oregon), and Scheie Eye Institute and the Children's Hospital of Philadelphia and the Hospital of the University of Pennsylvania (Philadelphia, Pennsylvania). Trial site personnel are listed below.

There were five experimental cohorts: three adult cohorts (1–3) receiving low-dose ($6\times10^{11}$ vg/mL), mid-dose ($1\times10^{12}$ vg/mL), or high-dose ($3\times10^{12}$ vg/mL) EDIT-101, and two pediatric cohorts (4–5) receiving mid-dose ($1\times10^{12}$ vg/mL) or high-dose ($3\times10^{12}$ vg/mL) EDIT-101. No participants have been enrolled in the pediatric high-dose cohort.

*Study eligibility*

All participants in cohort 1 (adult low-dose) were required to have best-corrected visual acuity (BCVA) of white field projection (WFP), black–white discrimination (BWD), or light perception (LP) in the study eye as assessed with the Berkeley Rudimentary Vision Test. BCVA of WFP, BWD, and LP were reassigned as 3.2, 3.5, and 3.9 logMAR, respectively. Sentinel participants in cohorts 2–5 were required to have BCVA of LP–1.6 logMAR in the study eye. Non-sentinel participants in cohorts 2–5 were required to have BCVA of LP–0.4 logMAR in the study eye. Participants were excluded if they had other known disease-causing mutations, a passing score for the most difficult Ora-Visual Navigation Challenge (VNC™) mobility course,

active systemic infection, active ocular infection/inflammation in either eye, history of steroid-responsive intraocular pressure with increases > 25 mm Hg in either eye, vaccination or immunization within 28 days of screening, inability or unwillingness to take oral prednisone, or prior gene therapy/oligonucleotide treatment. Additional information regarding study eligibility are included in the study protocol in **Supplementary Appendix 2**.

*Study treatment*

Participants underwent a standard pars plana vitrectomy and received a single subretinal injection of up to 300 µL of EDIT-101 in the study eye. Cohort 1 (adult low-dose) received $6\times10^{11}$ vg/mL of EDIT-101, cohort 2 (adult mid-dose) received $1\times10^{12}$ vg/mL of EDIT-101, cohort 3 (adult high-dose) received $3\times10^{12}$ vg/mL of EDIT-101, and cohort 4 (pediatric mid-dose) received $1\times10^{12}$ vg/mL of EDIT-101. Intra-operative optical coherence tomography (OCT) was used to guide delivery of EDIT-101 to the subretinal space between the retinal pigment epithelium (RPE) and the photoreceptor layer in most cases. Subretinal injections covered the posterior pole of the retina and extended to the vascular arcades. All injections were performed using established surgical techniques[1,2] by three experienced surgeons (JIC, AKL and AMM).

*Study outcomes*

Safety of EDIT-101 was assessed through frequency and severity of treatment-related adverse events (AEs) related to EDIT-101, number of procedure-related AEs, and incidence of dose-limiting toxicities (DLTs). AEs were identified through physical, laboratory, and ophthalmic assessments. Non-ocular severe AEs that occurred at or before the week 6 visit for sentinel participants, and at or before the week 4 visit for non-sentinel participants were assessed by the investigator as being related to the study drug.

Immune response to the EDIT-101 AAV5 capsid and SaCas9 was evaluated in participants' peripheral blood mononuclear cells, serum, and plasma using an interferon-γ enzyme-linked immuno spot assay (ELISA). An electrochemiluminescence immunoassay was used to detect binding antibodies (BABs) to AAV5 and SaCas9 in serum, and a cell-based virus neutralization assay was used to detect AAV5 neutralizing antibodies (nABs) in plasma. The limit of sensitivity for the screening assay for BABs to SaCas9 was 40.9 ng/mL, and the limit of sensitivity of the confirmatory assay was 24.2 ng/mL. EDIT-101 viral shedding was determined by quantifying vector genomes within blood, tears, nasal mucosa, and semen samples with a quantitative polymerase chain reaction assay targeting the SaCas9 transgene. Immunogenicity and viral shedding assays were validated to establish linearity, reproductivity, limits of detection, biological matrix effects, and acceptance criteria for detection of an immune response to AAV5 and SaCas9 or quantification of EDIT-101 viral genomes.

*Study assessments*

BCVA was assessed using the Early Treatment Diabetic Retinopathy Study (ETDRS) chart,[3,4] the LEA Symbols 15 Line Pediatric Eye Chart, and the Berkeley Rudimentary Visual Test.[5] Dark-adapted full-field stimulus testing (D-FST) sensitivity to blue, white, and red light was assessed using the Espion Ganzfeld Profile E3 ERG machine V6.0 (Diagnosys LLC; Massachusetts, United States).[6-8] Briefly, participants were dilated and dark-adapted for 45 minutes prior to testing with blue (448 nm peak wavelength), red (627 nm peak wavelength) and white light (white 6500 K using red, blue, and green light emitting diodes). FST assessments were repeated three times per stimulus and were considered reliable when at least one assessment had a quality metric > 1. The sensitivity output was the mean of all reliable assessments. Dark-adapted cone-mediated sensitivity loss was estimated as the difference between the sensitivity

determined with the red stimulus in study participants and the mean sensitivity measured at the cone plateau phase of the dark adaptation function in normal participants.[8-10]

Visual function navigation was assessed using the Ora–VNC™ (VNC), a four-course, multi-luminance mobility challenge (Supplementary figure 4). The first course is the Backlit Room Exit (BRE), which contains two illumination levels scored from 1–2, the second is the High Contrast Room Exit (HCRE)—a straight course with high contrast obstacles and three illumination levels scored from 3–5. The penultimate course is the High Contrast Visual Navigation Challenge (HCVNC), which comprises several turns, high contrast obstacles, and eight illumination levels scored from 6-13. The final course is the Low Contrast Visual Navigation Challenge (LCVNC), which contains several turns, low contrast obstacles, and eight illumination levels scored from 14-21.

VNC assessment at each scheduled visit was performed across multiple luminance levels. Each eye was tested separately. On the first day of the assessment (screening visit), the participant was assessed on all courses at all luminance levels starting from the most difficult course (LCVNC) and the dimmest light level (0.35 lux). The first course that was successfully navigated ("passed") by the participant based on prespecified rules (for example, keeping to the path of the course, hitting less than pre-defined number of obstacles, and completing the course within a time limit) was noted and became the reference point for subsequent testing. At each new study visit, the assessment started at three light levels dimmer than that passed on the previous visit and was increased until the participant passed the course.

During the course assessment, a video film of the assessment was acquired in night mode using infrared light to mask the luminance level of the assessment. The video recording of the assessment was sent to the vendor reading center for masked scoring. The assessment for each

light level was performed once and so the scores were not averaged. The grade of the VNC was defined based on the course and luminance level at which the navigation assessment was passed. The lux luminance levels of the courses were: BRE – 10% and 100% of the maximum luminance of the illumination source and obstacles; HCRE – 1 lux, 22 lux and 500 lux; LCVNC and HCVNC – 0.35 lux, 1 lux, 3 lux, 8 lux, 22 lux, 63 lux, 178 lux and 500 lux.

Spectral domain optical coherence tomography (OCT) images of the central retina were obtained using Heidelberg Spectralis instruments following standard clinical procedures (Heidelberg Engineering; Heidelberg, Germany).[11] Measurements of retinal structure including total retinal thickness, foveal outer nuclear layer (ONL) thickness, and ellipsoid zone width were obtained from horizontal cross-sectional B-scans through the fovea for participants for whom image quality was sufficient to permit these measurements.[12,13] Images were independently assessed and graded to ensure uniformity.

Transient pupillary light reflex (TPLR) responses were elicited using the PLR-3000 pupilometer (Neuroptics, Irvine, CA) using a 0.33 second white stimulus at the lowest intensity available (10μW). Since perception in these patients was assumed (and confirmed in this study) to be mainly cone photoreceptor mediated, direct TPLRs were obtained after five minutes of dark adaptation, alternating between each eye, starting with the right eye. The pupil diameter was calculated and plotted as a function of time after presentation of the stimulus by the pupilometer software. The TPLR amplitude was defined as the difference between the starting pupil diameter and pupil diameter measured at 0.6s after stimulus presentation, as validated for patients with severe early-onset retinal degeneration.[14,15] Efficacy limits for TPLR were based on thresholds established from the limits of the variability (mean ± 2SD) of the intervisit differences in the

untreated contralateral eyes. The variability estimates are consistent with reported short-term intervisit variability of the TPLR in this disease with similar methodology.[13]

**Supplementary Information**

*Additional assessments*

The additional psychophysical assessments below were considered exploratory and were planned in hopes that patients with milder phenotypes would be able to reliably complete the tests, but were anticipated to be of limited use in patients with typical severe vision loss who participated in this initial phase of the BRILLIANCE trial.

Kinetic Visual Field Testing

Kinetic visual field testing was performed using the Octopus 900 perimeter (Haag-Streit, Bern Switzerland) using the V4e, III4e, and I4e target stimuli.[16] Seven participants were able to perform the test to some degree. The other seven were unable to perform the test due to nystagmus or poor vision. Of the seven participants who were able to perform field testing, only two (C3P2, C3P5) were able to complete the test by only using the largest target (V4e stimulus) in both eyes at more than one visit. Neither of these participants showed a change in visual field area up to 12 months post-treatment.

Contrast Sensitivity

Contrast sensitivity testing using the Pelli-Robson chart was performed for the four participants with BCVA of 1.0 logMAR or better (C2P3, C2P4, C3P2, C3P4).[17] The score is the log sensitivity of the faintest triplet in which two of the three letters were identified correctly. All four participants had baseline scores worse than 1.2, consistent with moderate to severe visual impairment. No change in contrast sensitivity from baseline was observed.

Color Vision

Farnsworth D-15 color vision testing was performed for eyes with BCVA of 1.0 logMAR or better.[18] Baseline and last-visit assessment data are available for the study eyes of three participants (C2P3, C2P4, C3P2). The score is the number of caps placed correctly. All three participants had abnormal color vision at baseline with multiple major crossings without a specific axis of confusion. No reproducible change in color vision from baseline was observed.

Patient/Caregiver Global Impression of Change

The Global Impressions of Change was administered by asking participants about the change in their vision problem over the past seven days. Caregivers responded to the questions for the two pediatric participants. This assessment was not performed at baseline, so it is not possible to interpret the data from the latest assessment with regard to the effects of the EDIT-101 treatment.

*Author Contributions*

The BRILLIANCE trial was designed by Editas Medicine, with assistance from members of the study team and investigators at the trial sites (JC, AL, MP, EP). Investigators at the trial sites gathered the clinical data, and investigators at Editas Medicine gathered and analyzed the immunology data. Investigators from Editas Medicine and the trial sites analyzed the clinical data, vouch for all the data and analyses, and decided to publish this research. Dr. Shervonne Poleon from Porterhouse Medical prepared the initial draft of the manuscript and assisted with revisions. All work from Porterhouse Medical was sponsored by Editas Medicine. Investigators from Editas Medicine and the trial sites (BSA, TA, KK, MP, EP) revised the original manuscript

and addressed concerns raised by the reviewers. All investigators from the trial sites have clinical trial agreements with the study sponsor—Editas Medicine, which include confidentiality clauses.

**Figure S1.** CEP290 Protein Localization

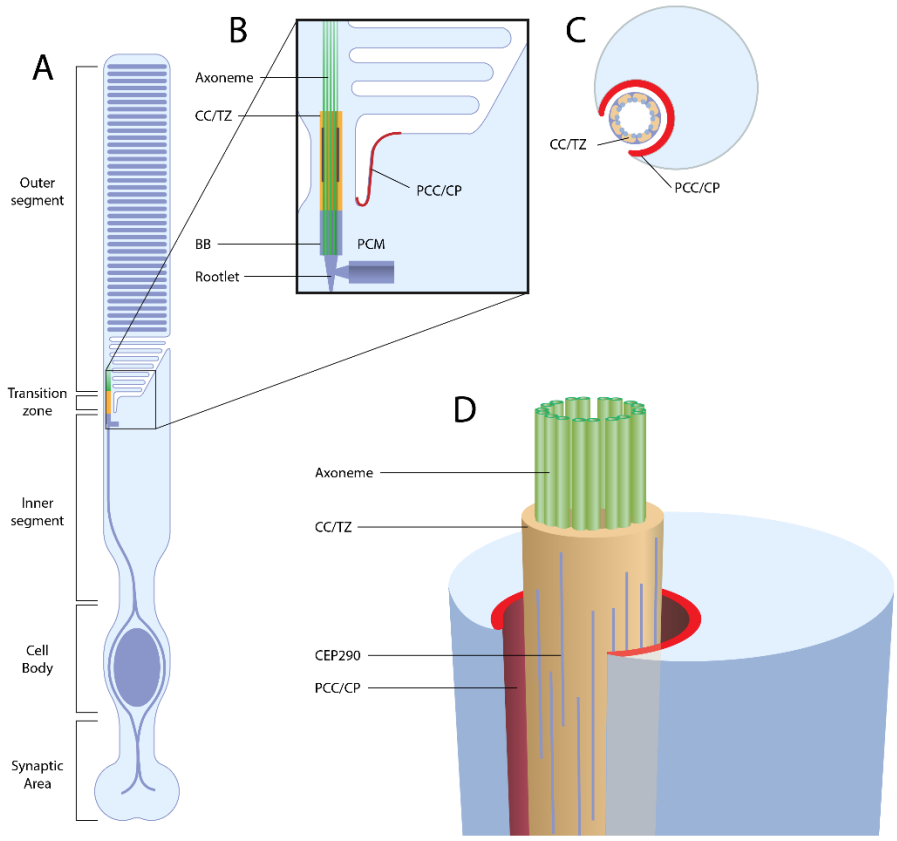


**Schematic of CEP290 protein localization. A.** Schematic of a rod photoreceptor, showing specialized domains. **B.** Enlargement of the rod photoreceptor transition zone: axoneme (green), connecting cilium/transition zone (CC/TZ; orange), basal body (BB; purple), periciliary complex or ciliary pocket (PCC/CP; red). **C.** Cross section through the CC/TZ. **D.** Three-dimensional representation of the transition zone and adjacent domains showing possible position of CEP290. This figure has been adapted from the figure entitled *Four distinct compartments in photoreceptor primary cilia, indicating known proteins that define their respective extent* by Rachel et al. (2012).[19] License: Rightslink® by Copyright Clearance Center

**Figure S2.** EDIT-101 Design

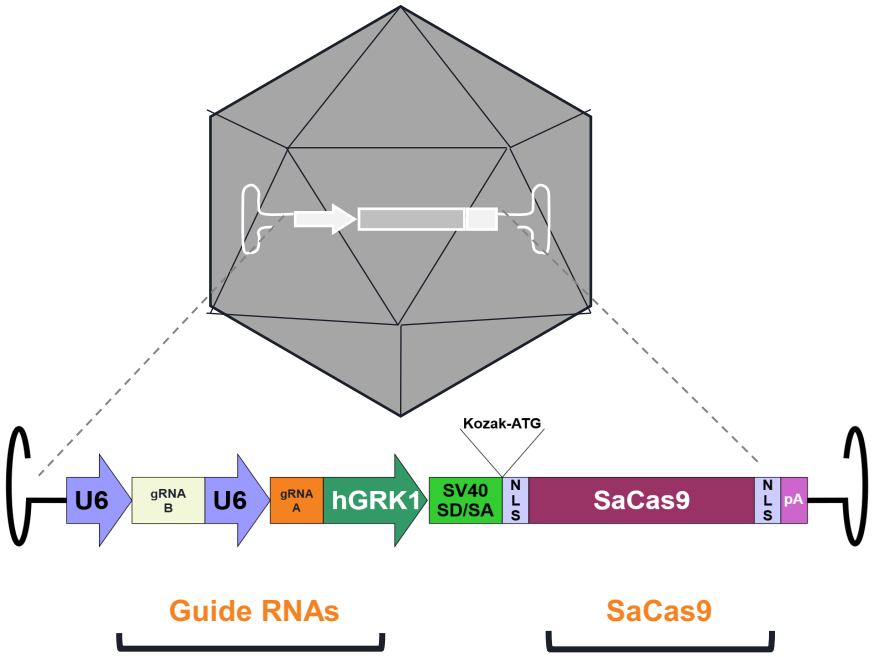


**Schematic representation of EDIT-101, an AAV5 viral vector containing indicated components.** U6, human U6 polymerase III promoter; gRNA, guide ribonucleic acid; hGRK1, human G protein-coupled receptor kinase 1 promoter; SV40 SD/SA, simian virus 40-splice donor and splice acceptor containing intronic sequence; Kozak-ATG, consensus kozak sequence and ATG start codon; NLS, nuclear localization signal; SaCas9, Staphylococcus aureus Cas9; pA, polyadenylation signal.

**Figure S3.** BRILLIANCE Trial Design

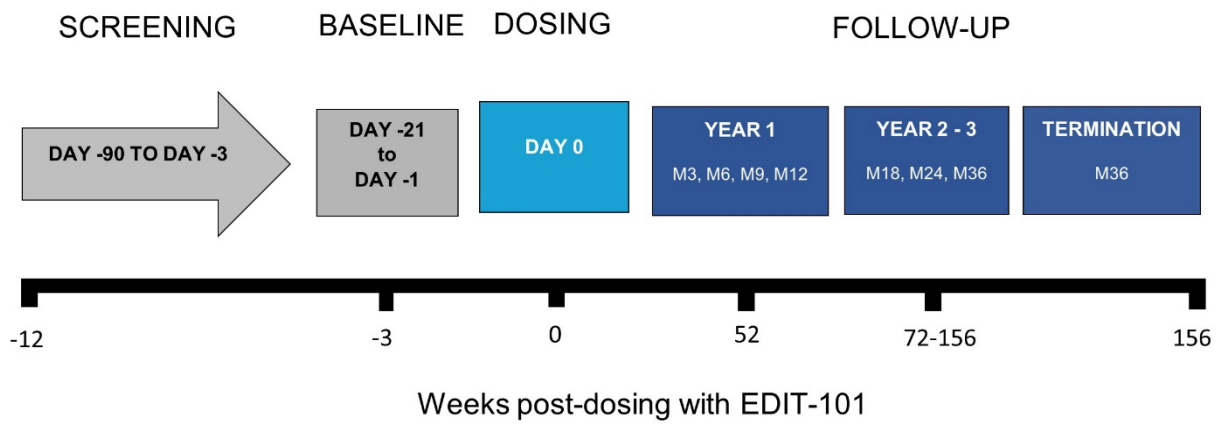


`

**BRILLIANCE trial design.** After a 3-month screening period, participants received a single subretinal injection of EDIT-101 in the worse-seeing (study) eye. Participants were monitored every three months for 1 year (M3, M6, M9, and M12), and then less frequently for an additional two years (M18, M24, M36). M, month.

**Figure S4.** Ora–VNC™ Mobility Course Challenge


**Four courses of the Ora—Visual Navigation Challenge (VNC) and relative assigned scores.**

**Figure S5.** CONSORT Diagram for BRILLIANCE Trial

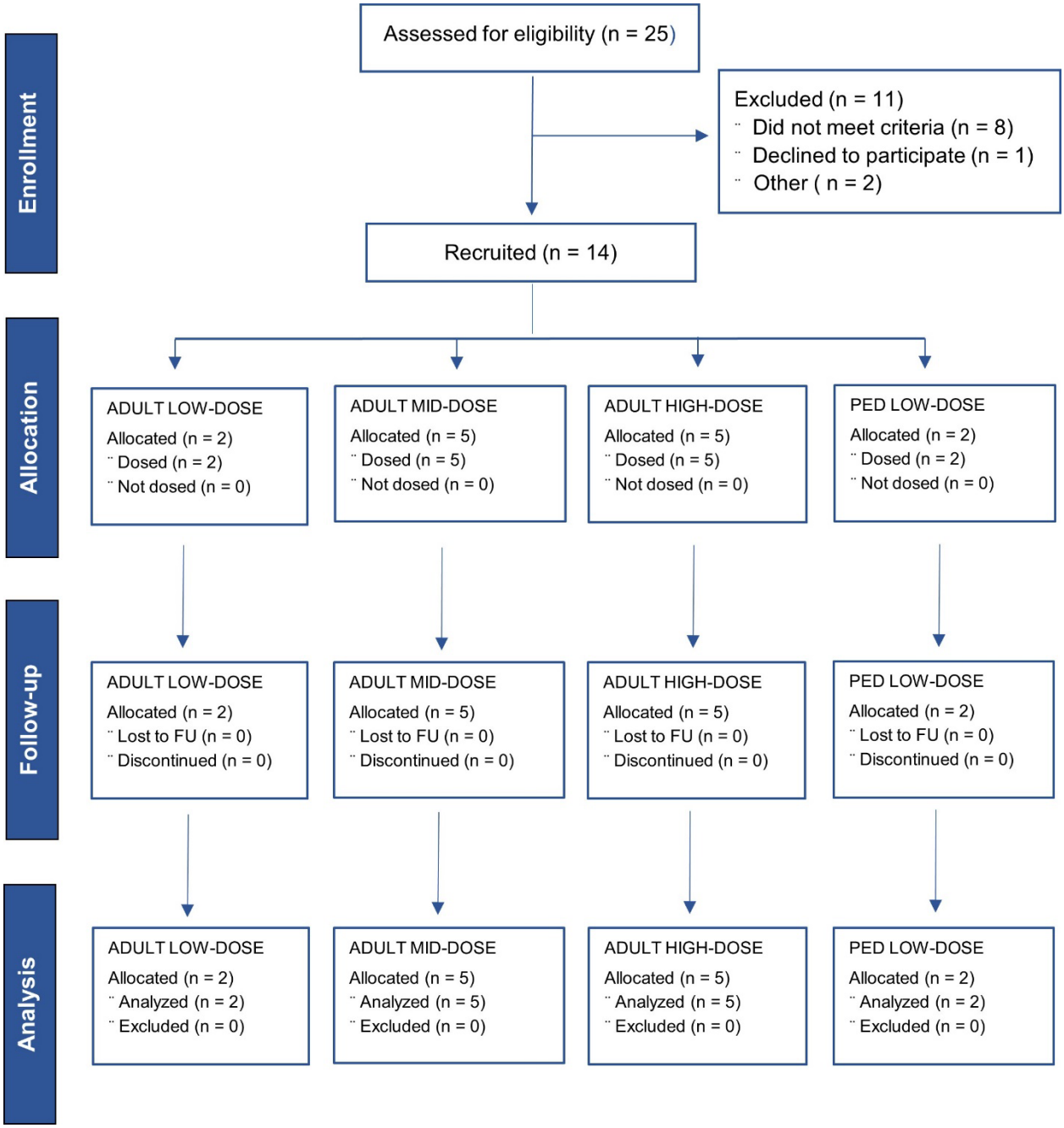


**CONSORT diagram indicating study enrollment, allocation, follow-up, and analysis.** Due to circumstances unrelated to the BRILLIANCE trial, the sponsor suspended enrollment after these 14 participants. FU, follow-up; Ped, Pediatric.

**Figure S6.** Treatment and Follow-up Status for Trial Participants

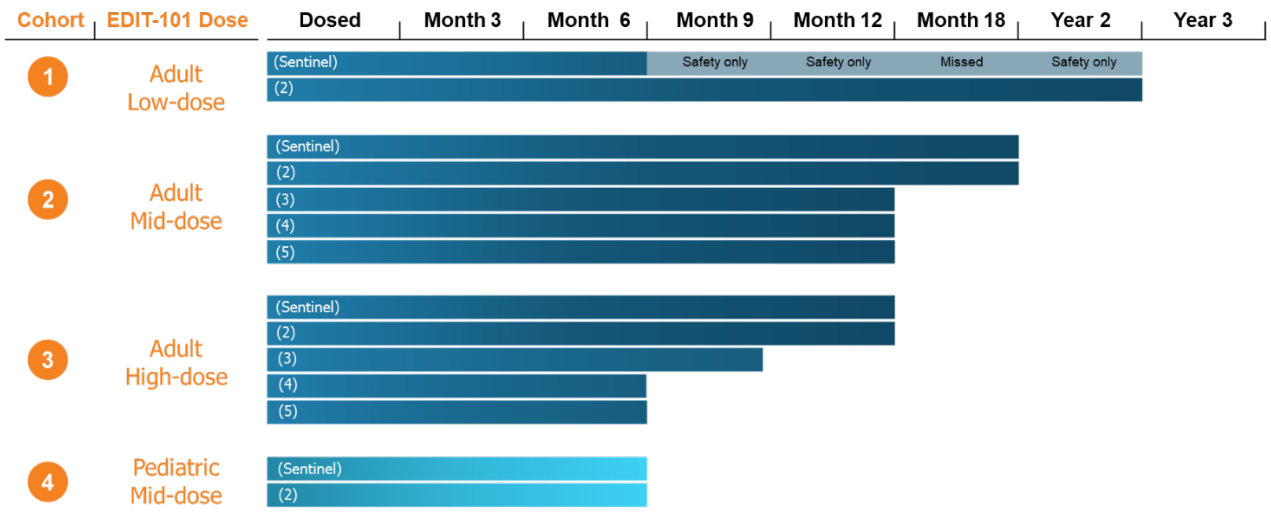


**Duration of safety and efficacy data for study participants.** Due to circumstances unrelated to the BRILLIANCE trial, the sponsor suspended enrollment after these 14 participants.

**Figure S7.** Subretinal Hyperreflective Mounds on OCT after Treatment

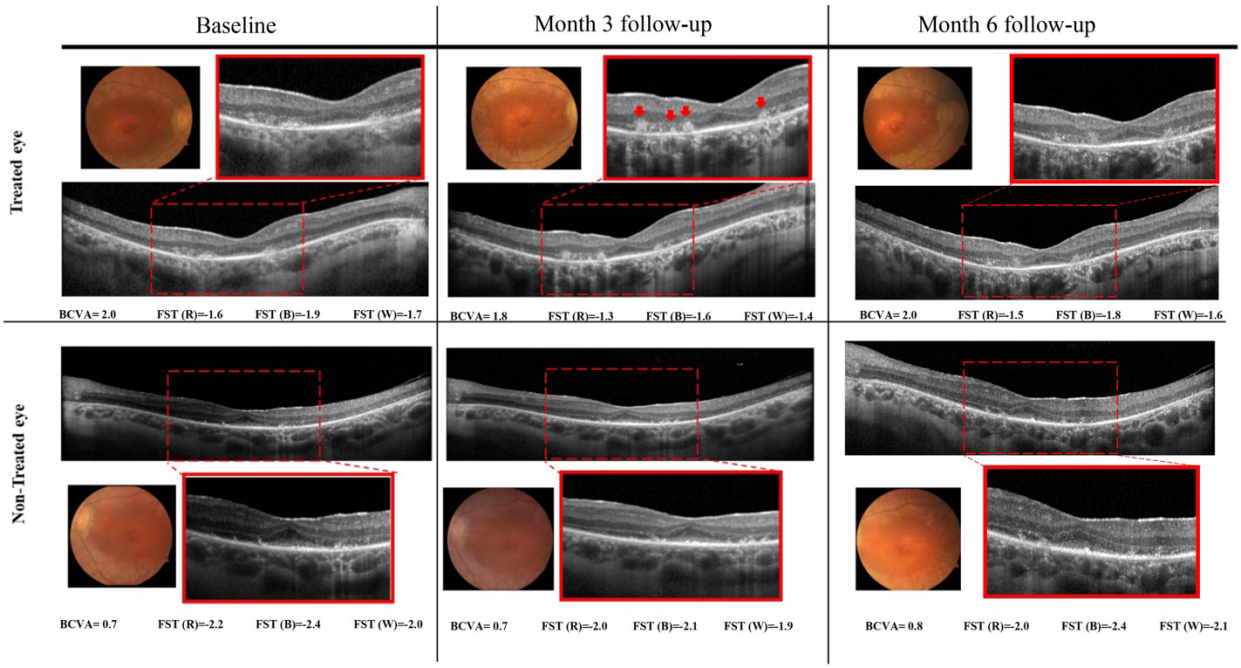


**Cross-sectional retinal images acquired with OCT.** Study (treated) versus contralateral (non-treated) eye of a participant (C3P4) who developed hyperreflective retinal mounds. The mounds (red arrows) were apparent at month 3 post-treatment and self-resolved (without steroid treatment) by month 6. BCVA, Best-corrected visual acuity; FST, full-field stimulus testing; OCT, Optical coherence tomography.

**Figure S8.** Retinal Pigment Epitheliopathy after Treatment

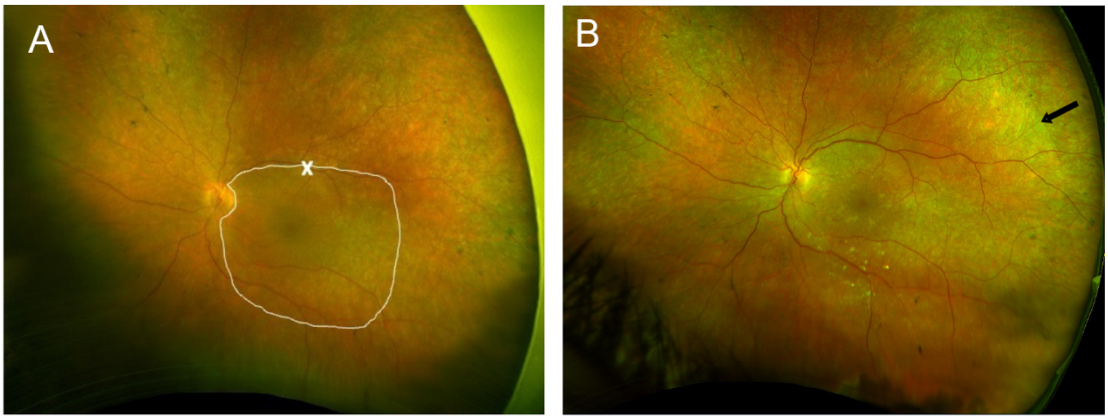


**Fundus photos of participant C2P5. A.** Baseline photo of treated (study) eye (left) showing approximate area of bleb following sub-retinal injection (white outline), with the injection site indicated (X). **B.** Fundus photo 6 months after treatment showing slightly lighter retinal pigment epithelium (RPE) pigmentation in the area of treatment (demarcation line indicated with arrow). The white spots/deposits noted below the fovea resolved at subsequent exams, while the change in RPE pigmentation has persisted in the same location. The RPE changes were not associated with changes in photoreceptor function or vision in these participants, as has been reported for RPE changes observed following other retinal gene therapy treatments, such as Luxturna.[20] C, cohort; P, participant; RPE, retinal pigment epithelium.

**Figure S9.** Viral Shedding in Tear and Blood Samples

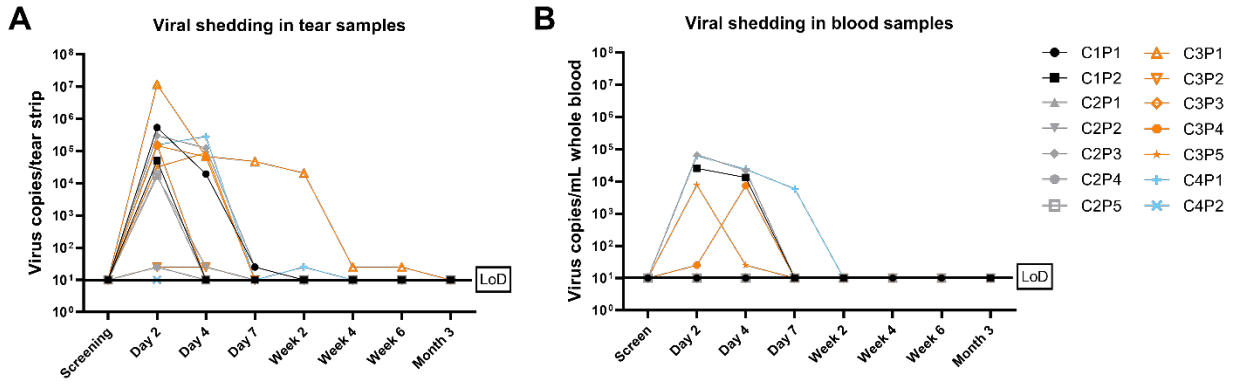


**Viral shedding assessed in tear samples collected from the treated eye and blood samples.**

**A.** Tear samples were collected from inside the lower eyelid of both the treated (study) and untreated (contralateral) eye. The highest quantity of viral genomes was observed 2-days post EDIT-101 administration and viral clearance was achieved by day 7 for most participants. **B.** Blood samples collected 2-days post EDIT-101 administration contained the highest observed quantity of viral genomes and viral clearance was achieved by day 7 for most participants. C, cohort; LoD, Limit of detection; P, participant.

**Figure S10.** Immune Response to AAV5 and SaCas9

**A**

| Participant | AAV5 Response | | SaCas9 Response | |
|---|---|---|---|---|
| | Pre | Post | Pre | Post |
| C1P1 | No | No | No | No |
| C1P2 | Yes | Yes | No | No |
| C2P1 | No | No | No | No |
| C2P2 | No | Yes | No | No |
| C2P3 | No | No | No | No |
| C2P4 | Yes | Yes | No | No |
| C2P5 | Yes | Yes | No | No |
| C3P1 | Yes | Yes | Yes | Yes |
| C3P2 | NC | Yes | NC | No |
| C3P3 | Yes | Yes | Yes | Yes |
| C3P4 | Yes | Yes | No | No |
| C3P5 | Yes | No | Yes | No |
| C4P1 | Yes | Yes | Yes | No |
| C4P2 | Yes | No | Yes | No |

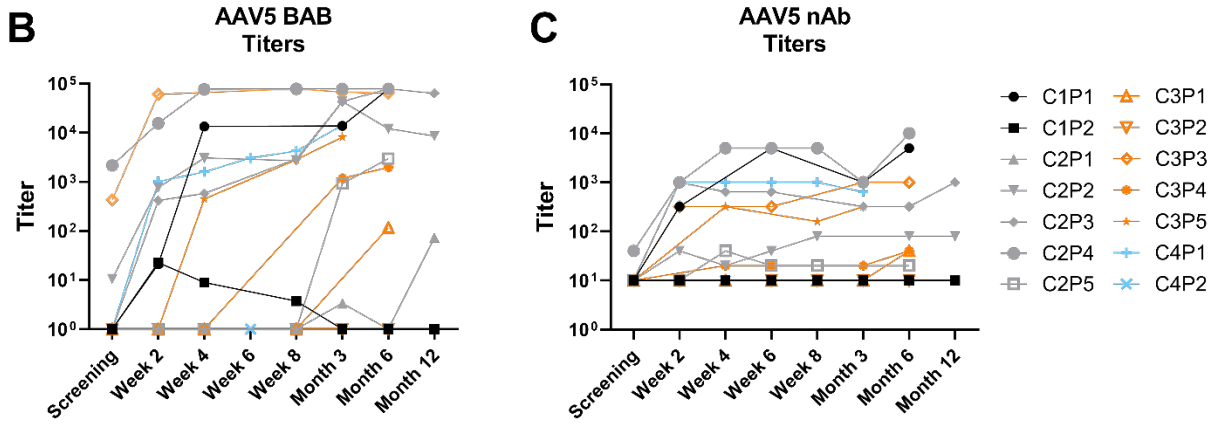


**Assessment of the innate and adaptive immune response to AAV5 and SaCas9. A.** The innate immune response to AAV5 and SaCas9 was assessed pre- and post-EDIT-101 administration. Most participants with a pre-existing innate immune response also had a post-treatment response. **B-C.** The adaptive immune response to AAV5 was assessed by measuring BAB and nAB levels pre- and post-EDIT-101 administration. AAV, adeno-associated virus; BAB, binding antibodies; C, cohort; nAB, neutralizing antibody; NC, not collected; P, participant; SaCas9, Staphylococcus aureus Cas9.

**Figure S11.** Change from Baseline in BCVA.

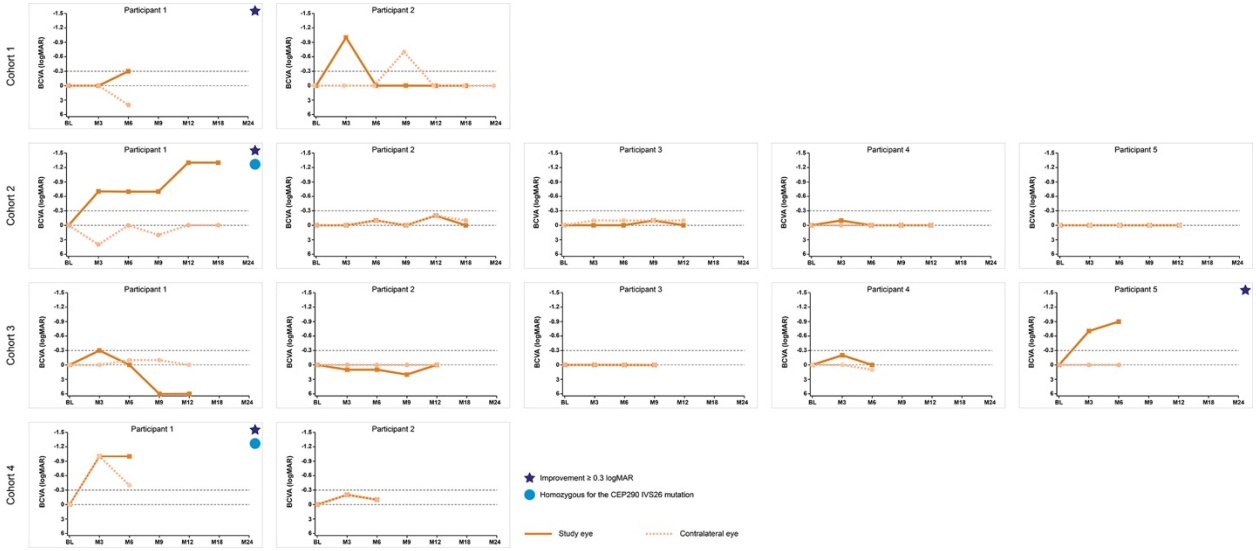


**Change from baseline for all participants.** As indicated, asterisks denote participants who demonstrated meaningful improvement based on the pre-specified criteria described in the manuscript. BCVA, best-corrected visual acuity; BL, baseline; CEP290, centrosomal protein 290; M, month.

**Figure S12.** Change from Baseline in FST Sensitivity.

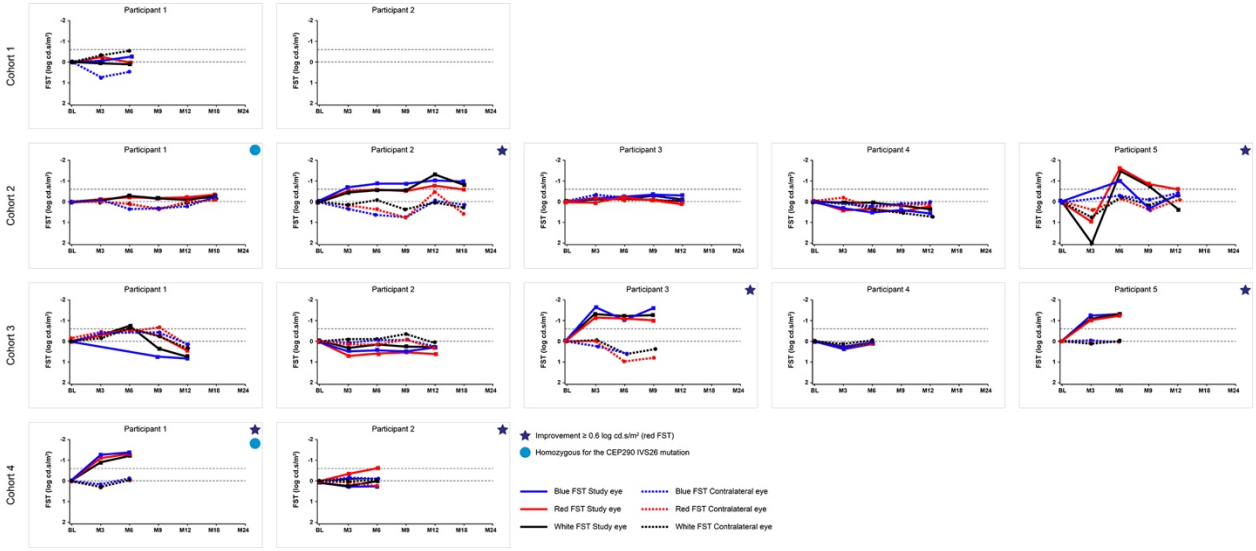


**Change from baseline for all participants.** As indicated, asterisks denote participants who demonstrated meaningful improvement based on the pre-specified criteria described in the manuscript. BL, baseline; CEP290, centrosomal protein 290; FST, full-field stimulus testing; M, month.

**Figure S13.** Change from Baseline in VNC Mobility Score.

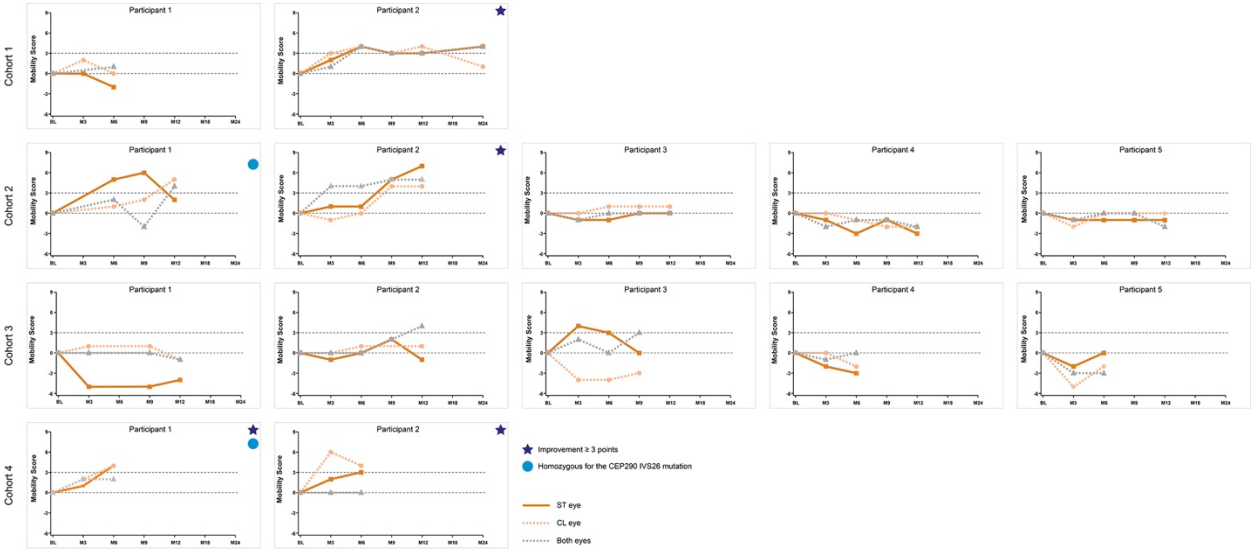


**Change from baseline for all participants.** As indicated, asterisks denote participants who demonstrated improvement based on the pre-specified criteria described in the manuscript. BL, baseline; CEP290, centrosomal protein 290; M, month; VNC, Visual Navigation Challenge.

**Figure S14.** Change from Baseline in Vision-related QoL.

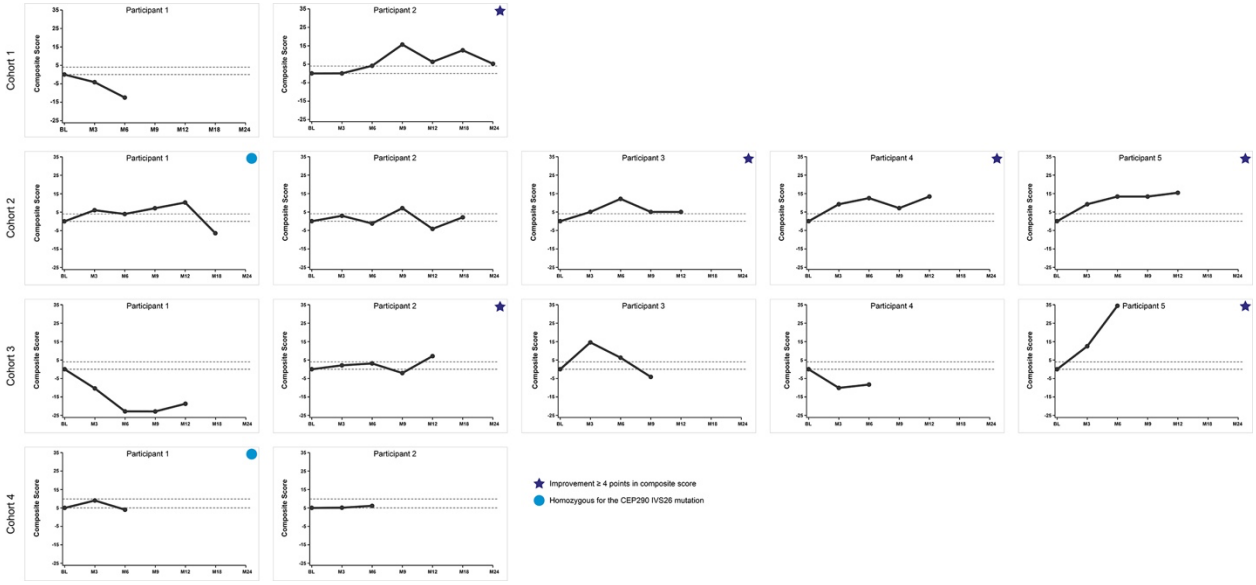


**Change from baseline for all participants.** As indicated, asterisks denote participants who demonstrated improvement based on the pre-specified criteria described in the manuscript. BL, baseline; CEP290, centrosomal protein 290; M, month; QoL, quality of life.

**Figure S15.** Transient pupillary light reflex responses

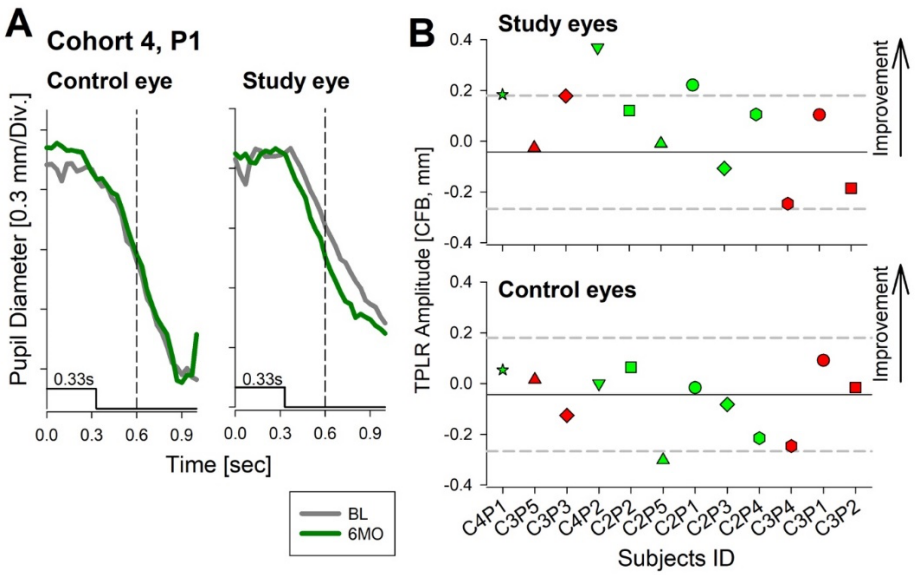


**Direct transient pupillary light reflex (TPLR) responses of clinical trial participants. A)** Traces of mean pupillary diameter as a function of time after a brief (0.3 second) white full-field light flash in a representative participant at baseline (gray traces) and 6 months after treatment (green traces) in the untreated control and treated study eye. The stimulus marker and scale bar are shown at the bottom. **B)** Change from baseline in TPLR constriction amplitudes in study versus control eyes in participants with evaluable TPLRs and FST results. TPLR amplitudes are defined as the difference between the baseline pupil diameter (gray traces) and the pupil diameter measured at a fixed time (0.6s) after stimulus presentation (vertical dashed line in panel A).[14,15] Horizontal solid lines represent the mean inter-visit differences (follow-up – baseline = -0.4 mm) of TPLR amplitudes in untreated eyes for this consensual (bilateral) reflex.[13] Horizontal dashed lines represent the limits of the variability (mean ± 2SD; SD = 0.11 mm) of this parameter. Variability estimates are consistent with previous reports using similar methodologies in *CEP290*-LCA.[13] Participants are sorted left to right in decreasing order of their sensitivity gains

by FST after treatment in the treated eyes, as shown in Figure 1. Colored symbols represent mid- (*green*) and high-dose (*red*) groups, with the same shapes for each participant as used in Figure 2. BL, baseline; CFB, change from baseline; M, month; FST, full-field stimulus testing; TPLR, transient pupillary light reflex.

**Supplementary Video 1.** Subretinal Delivery of EDIT-101

A representative excerpt from the surgical procedure is shown in Supplementary video 1, which shows injection of EDIT-101 into the subretinal space (left), as confirmed by intraoperative cross-sectional OCT imaging (right). The OCT images correspond to the blue lines shown in the surgical video. The formation of the subretinal bleb of injected EDIT-101 can be observed in the top two OCT images, while the retina in the bottom image is outside the bleb area. OCT, Optical coherence tomography.

**Table S1.** Demographic Characteristics of Patients with *CEP290*-associated Inherited Retinal Degeneration

| Demographic Characteristics | Population Distribution |
|---|---|
| Age | • *CEP290*-associated Inherited Retinal Degeneration (IRD) often manifests as early as the second year of life.[21]<br>• Based on research in this clinical population, patient age ranges from 2 months to 57 years.[22,23] Age at diagnosis ranges from < 1 year to 4 years.[24-26]<br>• In a study among adults and children with pathogenic variants in the *CEP290* gene, patients were found to present with a normal fundus at diagnosis (mean age = 1.9 years), with a marbleized fundus appearing in the first to second decade (mean age = 5.9 years) followed by pigmentary retinopathy (mean age = 19.7 years).[25]<br>• End-stage retinal degeneration was found to occur between the ages of 8 and 40 years in patients with *CEP290* mutations.[27] |
| Sex | • Based on research in this clinical population, females were found to constitute 38-55% of the population compared to 45-62% for males.[13,23,25] |
| Race and ethnicity | • The intronic c.2991+1655A.G mutation is the most prevalent mutant allele and is reported in 20% to 57% of patients of European descent.[21,23,25,28,29]<br>• *CEP290* mutations are prevalent in northwestern Europe, but contribute to only a minor part in Italy, Saudi Arabia, Spain, Southern India, and Korea.[21,27] |
| Representativeness of sample | • Achieving perfect representativeness can be challenging, and investigators must often balance practical constraints with the goal of obtaining a sample that reflects the population of interest. However, we believe that our study sample is representative of the wider clinical population. Participant age ranged from 9-63 years, females constituted 64% of the sample (9/14), and 100% of participants identified as non-Hispanic White. As such, this sample reflects the wider clinical population, which is largely of European descent, fairly equally distributed between males and females, and inclusive of a wide age spectrum. |

**Table S2.** OCT Measurements

| Participant ID | Treated Eye | ONL Thickness [foveal center, um] | | | | ONL Thickness [CFB, um] | |
|---|---|---|---|---|---|---|---|
| | | OD | | OS | | OD | OS |
| | | BL | FU | BL | FU | | |
| C1P1 | OD | 96 | NA | NA | NA | NA | NA |
| C1P2 | OD | 52 | 49 | 90 | 52 | -2.60 | -38.70 |
| | | | | | | | |
| C2P1 | OS | 76 | 88 | 70 | 88 | 11.62 | 18.06 |
| C2P2 | OD | 116 | 114 | 108 | 103 | -2.50 | -5.20 |
| C2P3 | OS | 137 | 134 | 139 | 129 | -2.58 | -10.40 |
| C2P4 | OS | 93 | 98 | 98 | 96 | 4.90 | -2.60 |
| C2P5 | OS | NA | NA | NA | 106 | NA | NA |
| | | | | | | | |
| C3P1 | OS | 48 | 43 | 52 | 45 | -5.17 | -6.45 |
| C3P2 | OD | 88 | 84 | 84 | 76 | -3.87 | -7.75 |
| C3P3 | OD | 96 | 108 | 114 | 93 | 12.91 | -20.65 |
| C3P4 | OD | 67 | 62 | 103 | 108 | -5.16 | 5.17 |
| C3P5 | OS | 77 | 75 | 103 | 93 | -2.58 | -10.32 |
| | | | | | | | |
| C4P1 | OD | 134 | 129 | 137 | 132 | -5.20 | 0.96 |
| C4P2 | OD | 129 | 116 | 121 | 124 | -13.00 | 1.02 |

The foveal ONL thickness was measured from OCT images obtained at the baseline and the latest follow-up visits. The normal range of foveal ONL thickness is estimated to be 111 +/- 15µm.[12] Green highlight indicates the treated eye. BL, baseline; C, cohort; CFB, change from baseline; FU, follow-up; NA, not available; OCT, optical coherence tomography; OD; right eye; ONL, outer nuclear layer; OS, left eye; P, participant; µm, micrometers.

**Table S3.** Change from Baseline in Key Efficacy Outcomes – Individual Participant Data

| Participant (Follow-up[M]) | Gender | Age | Zygosity | Baseline BCVA (ST eye) (logMAR) | Change from Baseline in Key Endpoints (Study Eye) | | | | | |
|---|---|---|---|---|---|---|---|---|---|---|
| | | | | | BCVA (logMAR) | Red FST (log cd.s/m²) | Blue FST (log cd.s/m²) | White FST (log cd.s/m²) | VNC mobility score | PRO[ǂ] score |
| **Cohort 1 – Adult low-dose** | | | | | | | | | | |
| Participant 1 (M6) | Female | 50 | CH | 3.5 | −0.3* | 0.0 | −0.3 | +0.1 | −2 | −13 |
| Participant 2 (M24) | Male | 42 | CH | 3.9 | 0 | NA | NA | NA | +4* | +5* |
| **Cohort 2 – Adult mid-dose** | | | | | | | | | | |
| Participant 1 (M18)[8] | Female | 54 | H | 2.7 | −1.3* | −0.4 | −0.3 | −0.3 | +2[∞] | −6 |
| Participant 2 (M18)[8] | Male | 20 | CH | 1.4 | 0 | −0.6* | −1.0* | −0.9* | +7* | +2 |
| Participant 3 (M12) | Female | 19 | CH | 0.6 | 0 | +0.1 | −0.3 | −0.1 | 0 | +5* |
| Participant 4 (M12) | Female | 63 | CH | 0.9 | 0 | +0.3 | +0.5 | +0.4 | −3 | +13* |
| Participant 5 (M12) | Female | 17* | CH | 3.9 | 0 | −0.6* | −0.3 | +0.3 | −1 | +15* |
| **Cohort 3 – Adult high-dose** | | | | | | | | | | |
| Participant 1 (M12) | Female | 28 | CH | 2.3 | +0.6 | +0.5 | +0.8 | +0.7 | −4 | -19 |
| Participant 2 (M12) | Female | 38 | CH | 1.0 | 0 | +0.6 | +0.3 | +0.3 | −1 | +7* |
| Participant 3 (M9) | Female | 36 | CH | 3.9 | 0 | −1.0* | −1.6* | −1.2* | 0 | −4 |
| Participant 4 (M6) | Male | 35 | CH | 2.0 | 0 | +0.1 | +0.1 | +0.1 | −3 | −8 |
| Participant 5 (M6) | Female | 59 | CH | 2.9 | -0.9* | −1.2* | −1.3* | −1.3* | 0 | +34* |
| **Cohort 4 – Pediatric mid-dose** | | | | | | | | | | |
| Participant 1 (M6) | Male | 14 | H | 3.9 | −1.0* | −1.3* | −1.4* | −1.2* | +4* | −1 |
| Participant 2 (M6) | Male | 9 | CH | 1.2 | −0.1 | −0.7* | +0.2 | 0.0 | +3* | +1 |

Change from baseline results at the longest follow-up visit. Please note that improvements in BCVA and FST are shown as negative values, while improvements in VNC and PRO are shown as positive values. Cohort 1 Participant 1 opted for follow-up visits at a non-trial site after 6 months of trial follow-up as a result of coronavirus disease policies implemented at the trial site; *Change from baseline is considered to be above the noise threshold and meaningful; [8]VNC data reported at M12, all other endpoints at M18; ∞≥ 3 change from baseline to M9; ǂCohort 1–3 – National Eye Institute Visual Function Questionnaire–25 composite score from: general vision, color vision, near vison, distance vision (change ≥ 4 considered meaningful in this analysis); cohort 4 – Children's Visual

Function Questionnaire composite score from: general vision, competence (change ≥ 4 considered meaningful in this analysis). BCVA, best-corrected visual acuity; CEP290, centrosomal protein 290; CH, compound heterozygous; FST, full-field stimulus testing (log cd.s/$m^2$); H, homozygous; M, month; ST, study; PRO, patient-reported outcome; VNC, Visual Navigation Challenge.

**Table S4.** Correlations between Efficacy Metrics

| Metric | Red FST | BCVA | VNC | PRO |
|---|---|---|---|---|
| **Red FST** | r=1 | tau=0.50<br>95% CI [0.07, 0.83] | r=-0.62<br>95% CI [-0.11, -0.87] | r=-0.36<br>95% CI [-0.76, 0.24] |
| **BCVA** | | tau=1 | tau=-0.36<br>95% CI [-0.75, 0.11] | tau=0.04<br>95% CI [-0.54, 0.62] |
| **VNC** | | | r=1 | r=0.13<br>95%CI [-0.64, 0.62] |
| **PRO** | | | | r=1 |

Pearson's correlation tests were used to examine pairwise correlations among Red FST, VNC, and PRO. Kendall's non-parametric correlation tests were used for comparing pairs involving BCVA because the BCVA values were not normally distributed. A bootstrap estimation was used to generate the confidence intervals for the Kendall's tau values. The data from the treated eyes of all participants at the latest assessment available was utilized. The analysis of correlation among these measures was post-hoc.

**Supplementary References**


1. Bennett J, Wellman J, Marshall KA, et al. Safety and durability of effect of contralateral-eye administration of AAV2 gene therapy in patients with childhood-onset blindness caused by RPE65 mutations: a follow-on phase 1 trial. Lancet 2016;388(10045):661-72. (In eng). DOI: 10.1016/s0140-6736(16)30371-3.
2. Gregori NZ, Davis JL. Surgical Observations from the First 120 Cases of Subretinal Gene Therapy for Inherited Retinal Degenerations. Retina 2020 (In eng). DOI: 10.1097/iae.0000000000003085.
3. Tsou BC, Bressler NM. Visual Acuity Reporting in Clinical Research Publications. JAMA Ophthalmol 2017;135(6):651-653. (In eng). DOI: 10.1001/jamaophthalmol.2017.0932.
4. Shamir RR, Friedman Y, Joskowicz L, Mimouni M, Blumenthal EZ. Comparison of Snellen and Early Treatment Diabetic Retinopathy Study charts using a computer simulation. Int J Ophthalmol 2016;9(1):119-23. (In eng). DOI: 10.18240/ijo.2016.01.20.
5. Bailey IL, Jackson AJ, Minto H, Greer RB, Chu MA. The Berkeley Rudimentary Vision Test. Optom Vis Sci 2012;89(9):1257-64. (In eng). DOI: 10.1097/OPX.0b013e318264e85a.
6. Klein M, Birch DG. Psychophysical assessment of low visual function in patients with retinal degenerative diseases (RDDs) with the Diagnosys full-field stimulus threshold (D-FST). Doc Ophthalmol 2009;119(3):217-24. (In eng). DOI: 10.1007/s10633-009-9204-7.
7. Roman AJ, Cideciyan AV, Aleman TS, Jacobson SG. Full-field stimulus testing (FST) to quantify visual perception in severely blind candidates for treatment trials. Physiol Meas 2007;28(8):N51-6. (In eng). DOI: 10.1088/0967-3334/28/8/n02.

8. Roman AJ, Cideciyan AV, Wu V, Garafalo AV, Jacobson SG. Full-field stimulus testing: Role in the clinic and as an outcome measure in clinical trials of severe childhood retinal disease. Prog Retin Eye Res 2022;87:101000. (In eng). DOI: 10.1016/j.preteyeres.2021.101000.
9. Collison FT, Park JC, Fishman GA, McAnany JJ, Stone EM. Full-Field Pupillary Light Responses, Luminance Thresholds, and Light Discomfort Thresholds in CEP290 Leber Congenital Amaurosis Patients. Invest Ophthalmol Vis Sci 2015;56(12):7130-6. (In eng). DOI: 10.1167/iovs.15-17467.
10. Collison F, Fishman G, McAnany JJ, Zernant J, Allikmets R. Psychophysical Measurement of Rod and Cone Thresholds in Stargardt Disease with Full-Field Stimuli. Investigative Ophthalmology & Visual Science 2013;54(15):3027-3027.
11. Sayman Muslubas I, Karacorlu M, Arf S, Hocaoglu M, Ersoz MG. Features of the Macula and Central Visual Field and Fixation Pattern in Patients with Retinitis Pigmentosa. Retina 2018;38(2):424-431. DOI: 10.1097/IAE.0000000000001532.
12. Aleman TS, Han G, Serrano LW, et al. Natural History of the Central Structural Abnormalities in Choroideremia: A Prospective Cross-Sectional Study. Ophthalmology 2017;124(3):359-373. (In eng). DOI: 10.1016/j.ophtha.2016.10.022.
13. Jacobson SG, Cideciyan AV, Sumaroka A, et al. Outcome Measures for Clinical Trials of Leber Congenital Amaurosis Caused by the Intronic Mutation in the CEP290 Gene. Invest Ophthalmol Vis Sci 2017;58(5):2609-2622. (In eng). DOI: 10.1167/iovs.17-21560.
14. Krishnan AK, Jacobson SG, Roman AJ, et al. Transient pupillary light reflex in CEP290- or NPHP5-associated Leber congenital amaurosis: Latency as a potential outcome

measure of cone function. Vision Res 2020;168:53-63. (In eng). DOI: 10.1016/j.visres.2020.01.006.

15. Aleman TS, Jacobson SG, Chico JD, et al. Impairment of the transient pupillary light reflex in Rpe65(-/-) mice and humans with leber congenital amaurosis. Invest Ophthalmol Vis Sci 2004;45(4):1259-71. (In eng). DOI: 10.1167/iovs.03-1230.

16. Roman AJ, Cideciyan AV, Schwartz SB, Olivares MB, Heon E, Jacobson SG. Intervisit variability of visual parameters in Leber congenital amaurosis caused by RPE65 mutations. Invest Ophthalmol Vis Sci 2013;54(2):1378-83. DOI: 10.1167/iovs.12-11341.

17. Pelli DG, Bex P. Measuring contrast sensitivity. Vision Res 2013;90:10-4. DOI: 10.1016/j.visres.2013.04.015.

18. Vingrys AJ, King-Smith PE. A quantitative scoring technique for panel tests of color vision. Invest Ophthalmol Vis Sci 1988;29(1):50-63. (https://www.ncbi.nlm.nih.gov/pubmed/3257208).

19. Rachel RA, Li T, Swaroop A. Photoreceptor sensory cilia and ciliopathies: focus on CEP290, RPGR and their interacting proteins. Cilia 2012;1(1):22. (In eng). DOI: 10.1186/2046-2530-1-22.

20. Kiraly P, Cottriall CL, Taylor LJ, et al. Outcomes and Adverse Effects of Voretigene Neparvovec Treatment for Biallelic RPE65-Mediated Inherited Retinal Dystrophies in a Cohort of Patients from a Single Center. Biomolecules 2023;13(10). DOI: 10.3390/biom13101484.

21. Perrault I, Delphin N, Hanein S, et al. Spectrum of NPHP6/CEP290 mutations in Leber congenital amaurosis and delineation of the associated phenotype. Hum Mutat 2007;28(4):416. (In eng). DOI: 10.1002/humu.9485.

22. Cideciyan AV, Aleman TS, Jacobson SG, et al. Centrosomal-ciliary gene CEP290/NPHP6 mutations result in blindness with unexpected sparing of photoreceptors and visual brain: implications for therapy of Leber congenital amaurosis. Hum Mutat 2007;28(11):1074-83. (In eng). DOI: 10.1002/humu.20565.

23. McAnany JJ, Genead MA, Walia S, et al. Visual acuity changes in patients with leber congenital amaurosis and mutations in CEP290. JAMA Ophthalmol 2013;131(2):178-82. (In eng). DOI: 10.1001/2013.jamaophthalmol.354.

24. Testa F, Sodi A, Signorini S, et al. Spectrum of Disease Severity in Nonsyndromic Patients With Mutations in the CEP290 Gene: A Multicentric Longitudinal Study. Invest Ophthalmol Vis Sci 2021;62(9):1. (In eng). DOI: 10.1167/iovs.62.9.1.

25. Sheck L, Davies WIL, Moradi P, et al. Leber Congenital Amaurosis Associated with Mutations in CEP290, Clinical Phenotype, and Natural History in Preparation for Trials of Novel Therapies. Ophthalmology 2018;125(6):894-903. (In eng). DOI: 10.1016/j.ophtha.2017.12.013.

26. Sahli E, Kiziltunc PB, Idil A. A Report on Children with CEP290 Mutation, Vision Loss, and Developmental Delay. Beyoglu Eye J 2023;8(3):226-232. (In eng). DOI: 10.14744/bej.2023.37233.

27. Coppieters F, Lefever S, Leroy BP, De Baere E. CEP290, a gene with many faces: mutation overview and presentation of CEP290base. Hum Mutat 2010;31(10):1097-108. (In eng). DOI: 10.1002/humu.21337.

28. den Hollander AI, Roepman R, Koenekoop RK, Cremers FP. Leber congenital amaurosis: genes, proteins and disease mechanisms. Prog Retin Eye Res 2008;27(4):391-419. (In eng). DOI: 10.1016/j.preteyeres.2008.05.003.

29. den Hollander AI. Omics in Ophthalmology: Advances in Genomics and Precision Medicine for Leber Congenital Amaurosis and Age-Related Macular Degeneration. Invest Ophthalmol Vis Sci 2016;57(3):1378-87. (In eng). DOI: 10.1167/iovs.15-18167.